doi.org/10.36721/PJPS.2026.39.1.REG.14096.1

Development of ginkgolide B nanocrystals via miniaturized wet bead milling: A QbD approach

Yun Liu[1]*, Hengyu Xu[2], Meili Lu[3] and Hongxin Wang[3]

[1]Department of Pharmacy, Liaoning Vocational College of Medicine, Maple Leaf Road, Xihu District, Benxi, Liaoning, China
[2]Medical Mass Spectrometry Technology Innovation Center of Liaoning Province, Shenyang Harmony Health Medical Laboratory, No. 36, Nanping East Road, Hunnan District, Shenyang, Liaoning, China
[3]Key Laboratory of Cardiovascular and Cerebrovascular Drug Research of Liaoning Province, Jinzhou Medical University, Section 3, Songpo Road, Linghe Distric, Jinzhou, Liaoning, China

Abstract: **Background**: Ginkgolide B (GB), a potent platelet-activating factor antagonist with multi-faceted pharmacological effects, suffers from extremely low oral bioavailability due to poor aqueous solubility and permeability. While nanocarriers have been explored, nanocrystal technology offers a carrier-free strategy with ultrahigh drug loading. **Objectives**: This study aimed to develop an orally administrable GB nanocrystal (GB-NC) formulation using a Quality by Design (QbD) approach to enhance dissolution rate and absorption potential, while ensuring stability and scalability. **Methods**: GB-NC were fabricated via a miniaturized wet bead milling technique. Critical process parameters were optimized using a Box-Behnken design, with particle size, polydispersity index (PDI), and stability index as key quality attributes. Stabilizers were screened, and lyoprotectants were selected for freeze-drying. The optimized nanocrystals were characterized for morphology, crystallinity, in vitro dissolution, stability, and cellular permeability using MDCK cell monolayers. **Results**: The optimal formulation, stabilized with PVP K30 (0.51%) and soy lecithin (0.34%) and milled for 10 hours, yielded nanocrystals with a particle size of 82.4 ± 1.97 nm, a low PDI, and good stability. Freeze-drying with glycine/glucose preserved redispersion properties. The GB-NC demonstrated significantly enhanced dissolution (>90% within 20 min) in both simulated gastric and intestinal fluids compared to raw GB. Cellular permeability (P_{app}) increased significantly, and the freeze-dried product remained stable for 6 months at 4°C and 25°C. **Conclusion**: A QbD-guided miniaturized wet bead milling process successfully produced stable GB-NC with markedly improved dissolution and cellular permeability. This presents a promising and scalable strategy to overcome the delivery challenges of GB, laying a foundation for developing effective oral formulations to enhance its bioavailability.

Keywords: Ginkgolide B; Miniaturized wet bead milling technique; Nanocrystals; Oral absorption; Quality by Design

Submitted on 07-02-2025 – Revised on 15-04-2025 – Accepted on 01-07-2025

INTRODUCTION

Ginkgolide B (GB), a key bioactive component of Ginkgo biloba, functions as a natural antagonist of Platelet-Activating Factor (PAF) (Almutairi, Ullah *et al*., 2022). PAF, a phospholipid mediator, plays a critical role in inflammatory responses, thrombosis, and neurodegenerative diseases by activating platelets and leukocytes (Suzuki, Taketomi *et al*., 2025, Upton, Grunebaum *et al*., 2022). In addition to inhibiting platelet activation and preventing thrombosis, GB also exhibits various pharmacological effects, including anti-oxidation, anti-inflammation, anti-apoptosis, protection of the central nervous system, and protection of ischemic tissue (Feng, Sun *et al*., 2019, Gachowska, Szlasa *et al*., 2021). Despite this therapeutic potential, GB's clinical translation faces significant challenges: its extremely low aqueous solubility and poor intestinal permeability result in less than 20% oral bioavailability compared to intravenous administration (Aa, Fei *et al*., 2018, Madgula, Avula *et al*., 2010, Zekri, Boudeville *et al*., 1996). Some nanocarriers, such as polymer nanoparticles (Zhao, Xiong *et al*., 2020), nanoemulsions (Yang, Cai *et al*., 2014), and ginkgolide B-modified carbonized polymer dots (Yang, Wei *et al*., 2023), have been attempted to address these limitations but face inherent trade-offs between drug loading capacity, formulation stability, and scalability. Nanocrystal technology offers a paradigm shift by eliminating carrier materials while achieving ultrahigh drug loading through pure drug particle size reduction (Che, Fu *et al*., 2024, Lu, Li *et al*., 2016). These benefits have contributed to the approval of over 20 nanocrystal-based drugs, such as Cabenuva® (Taki, Soleimani *et al*., 2022) and Invega Hafyera® (Peters, Dyer *et al*., 2023). Although GB-NC have been prepared via the antisolvent precipitation method, the use of the organic solvent acetone poses a potential risk of solvent residue, and the resultant drug content is exceedingly low (0.4 mg/mL), rendering it arduous to meet the requirements of clinical application (Liu, Liu *et al*., 2020). In this study, GB-NC were successfully prepared using the miniaturized medium grinding method, which has been documented in our previous research (Liu, Zhang *et al*., 2024).

The miniaturized medium grinding method, characterized as a top-down approach, employs a small-volume glass vial

**Corresponding author:* e-mail: liuyun@lnvcm.edu.cn

as the grinding chamber. Magnetic stirring is used to induce rotational motion, which serves as the driving force for grinding. Zirconia beads, possessing specific volume and particle size, are employed as the grinding medium, facilitating the reduction of drug particles to the nanoscale through collision and shearing mechanisms. Comparative analysis among this method and the conventional ball mill grinding method and high-pressure homogenization method reveals that the miniaturized medium grinding method significantly minimizes drug consumption and experimental expenses, rendering it highly suitable for nanocrystal formulation screening in laboratory settings. Notably, the miniaturized medium grinding method has been shown to enable drug formulation screening, and the resulting formulations can subsequently be scaled up using the high-pressure homogenization method, provided appropriate process parameters are used. This scaling-up process has been demonstrated in some studies (Lestari, Müller *et al*., 2015, Liu, Yao *et al*., 2017, Romero, Keck *et al*., 2016).

Hence, given the pressing demand for the development of oral formulations of GB, this study aims to develop commercially viable oral GB-NC products through a systematic experimental design to improve the dissolution rate and oral bioavailability of GB.

MATERIALS AND METHODS

Materials

GB (purity ≥ 98%) was obtained from Hubei Jusheng Technology Co., Ltd. (Hubei, China). Soy lecithin powder (SL, 98%), hydroxypropyl methylcellulose E5 (HPMC E5), sodium dodecyl sulfate (SDS), sodium deoxycholate (SDC), Vitamin E-TPGS, Cremophor EL-35, Tween 80, polyethylene glycol 15-hydroxystearate (HS-15), glycyrrhizic acid (GA), mannitol, xylitol, maltose, glycine, and glucose were purchased from Shanghai Macklin Biochemical Technology Co., Ltd. (Shanghai, China). Polyvinylpyrrolidone K-30 (PVP K30), Poloxamer 188, and Poloxamer 407 were obtained from BASF Co., Ltd. (Shanghai, China). Yttrium-stabilized zirconia beads were purchased from Wuxi Jiuzhong New Materials Technology Co., Ltd. (Jiangsu, China). All other solvents and chemicals were of analytical grade. MDCK cells were obtained from Procell Life Sciences & Technology Co., Ltd. (Wuhan, China).

Downscaled wet bead milling technique for GB-NC

In this study, GB-NC were successfully prepared using the miniaturized medium grinding method. Following preliminary experiments, the basic parameters for GB-NC preparation were as follows: A 20 mL glass vial with a diameter of 27 mm and a height of 57 mm was used as the grinding chamber; a magnetic stir bar with dimensions of 6×20 mm (diameter × length) was used; the grinding liquid volume was 4 mL; zirconia beads were added as the grinding medium, with a total volume of 4 mL (liquid-to-bead volume ratio of 1:1); the grinding process was conducted in an ice-water bath within a temperature range of 4–8 °C. The experimental setup is depicted in Fig. 1.

Quality by design approach

Quality by Design (QbD) commences product development with the predetermined quality target product profile (QTPP) as the foundation. It then proceeds to implement quality risk management through the control of the critical quality attributes (CQAs) of the product, ultimately culminating in the formulation of a quality control strategy (Farooqi, Yousuf *et al*., 2020, Kuk, Ha *et al*., 2019). Consequently, integrating the QbD concept into the formulation and process optimization of GB-NC guarantees product quality right from the design stage. This paper presents the design of GB preparation with a high dissolution rate and stability to enhance the oral absorption of GB, along with the establishment of the relevant QTPP and CQAs. Following the preliminary experimental findings, a risk assessment was conducted on the critical process parameters (CPPs) that could impact the CQAs of GB-NC. The risk assessment results were categorized into three levels: high risk, medium risk, and low risk.

Prescreening studies of GB-NC

Particle size and polydispersity index

The particle size and polydispersity index (PDI) of GB-NC samples were assessed using the Zetasizer Nano ZS90 (Malvern Instruments Ltd., UK). After a 1000-fold dilution, the samples were loaded into the quartz cuvette for detection. Measurements were performed in triplicate. The temperature during detection was maintained at 25ºC, and the samples were allowed to reach equilibrium for 3 min.

Stability Index (SI)

An appropriate volume of GB-NC sample was taken to determine the particle size (PS_{sample}). Subsequently, the sample was centrifuged at 1500 rpm for 30 min, and the particle size of the supernatant ($PS_{supernatant}$) was determined. The stability index (*SI*) (Yue, Li *et al*., 2013) was calculated according to the following formula:

$$SI = PS_{supernatant} / PS_{sample}$$

The sample was measured simultaneously in triplicate, and the results were averaged. An *SI* value closer to 1 indicates greater stability of the sample.

Screening of stabilizers

The prescribed conditions for the experiment included a drug concentration of 20 mg/mL and a stabilizer concentration of 0.5% (w/v). The process involved using zirconia beads with a diameter of 0.3–0.4 mm as the grinding medium, magnetic stirring at a speed of 1000 rpm, and a grinding time of 4 hours. Additional preparation conditions can be found as described in Section 2.2 on GB-NC preparation. The effects of various stabilizers on GB-NC were assessed based on appearance, particle size, PDI, and stability at room temperature.

Process parameters

The concentration of GB was fixed at 20 mg/mL, and the stabilizer used was a combination of PVP K30 (0.5%, w/v) and soy lecithin (0.3%, w/v). GB-NC were prepared following the procedures outlined in Section 2.2. Changes in particle size of GB-NC were observed under different conditions, including different zirconia bead sizes of 0.08–0.12, 0.3–0.4, 0.4–0.6, and 0.6–0.8 mm and rotating speeds of 800, 1000, 1200, and 1400 rpm, respectively.

Experimental optimization of GB-NC

After excluding the stabilizer and basic process parameters, the present study focused on optimizing three factors that significantly influence the properties of GB-NC, namely the concentration of PVP K30 (X_1), the concentration of SL (X_2), and the grinding time (X_3). The optimization process employed a Box-Behnken design (Cheng, Yuan *et al*., 2020) with 3 factors and 3 levels, using the average particle size (Y_1), PDI (Y_2), and SI (Y_3) as indicators. The factor levels and target response values are presented in Table 1, where the GB concentration was fixed at 20 mg/mL.

Freeze-drying of GB-NC and screening of lyoprotectant

To enhance the long-term physical stability of the product, GB-NC underwent freeze-drying and were subsequently stored as a solid. Prior to use, the lyophilized preparation was reconstituted with a solvent and then dispersed to form the drug nanocrystal solution (Khan, Ansari *et al*., 2021). Initially, the GB-NC solution was dispensed into 10 mL glass vials, with a sample volume of 1 mL per vial. Subsequently, the samples were prefrozen at -80ºC for 12 hours and subjected to a freeze-drying process using a FD5-3T lyophilizer (Siemon Co., Ltd., USA), with a cycle duration of 24 hours (Liu, Galvanin *et al*., 2018). To achieve a product characterized by a smooth appearance, loose texture, and small particle size upon redispersion, the addition of a specific concentration of lyoprotectants is imperative (Mohammady, Mohammadi *et al*., 2020). An investigation was conducted to evaluate the protective effect of various lyoprotectants on GB-NC, with the appearance of lyophilized products, redispersion rate, and the ratio of particle size after redispersion to that before redispersion (SR) as evaluation criteria.

Characterization of optimized GB-NC

The zeta potential, particle size, and PDI of GB-NC were measured using the Zetasizer Nano ZS90 (Malvern Instruments Ltd., UK). Further details can be found in Section 2.4.1. The structure of the GB-NC solution was analyzed using a transmission electron microscope (TEM, FEI TECNAI G2F20; FEI Co., Ltd., USA). After dilution, the GB-NC solution was applied to copper grids, air-dried at room temperature, and subsequently examined under an acceleration voltage of 200 kV. The morphology of lyophilized GB-NC was examined using a field emission scanning electron microscope (SEM, ZEISS SIGMA 500; Carl Zeiss NTS GmbH, Germany). The dried powder was placed on a metal plate, coated with gold-palladium alloy via sputtering, and then observed at an acceleration voltage of 5 kV. The crystalline state was determined via powder X-ray diffraction (PXRD) analysis (D8 ADVANCE; Bruker Ltd., Germany). GB-NC were freeze-dried first and then examined over a 2θ range of 5°–60° at a scan rate of 0.02°/s.

LC-MS analysis

Chromatographic condition

The chromatographic analysis was conducted using an Agilent ZORBAX XDB-C18 column (2.1 × 50 mm, 5 μm). The mobile phase consisted of methanol (A) and water (B), with the following gradient elution program: 0.0–0.5 min, 40%A (v/v); 0.51–1.5 min, 80%A (v/v); 1.51–3.0 min, 40%A (v/v). The flow rate was set at 0.5 mL/min, and the column temperature was maintained at 30ºC. Injection volume was 5 μL.

Mass spectrum conditions

The electrospray ion source (ESI) was employed in negative ion mode. The dry gas temperature was set at 300ºC, and the dry gas flow rate was 8 L/min. The nebulizer pressure was set at 40 psi, and the sheath gas temperature was maintained at 350ºC. The sheath gas flow rate was set at 12 L/min. The capillary voltage was set at 3500 V. The quantitative analysis of parent ions and daughter ions, along with the corresponding collision voltage (m/z 423.4→367.3, 5 eV) was conducted in multiple reaction monitoring (MRM) mode (Zhao, Geng *et al*., 2015).

The behavior of in vitro dissolution

An adequate quantity of GB raw material powder, physical mixture, and GB-NC freeze-dried powder (equivalent to 20 mg GB) were placed into dialysis bags with a molecular weight cutoff (MWCO) of 3.5 kDa. The ends of the bags were securely tied. Subsequently, these bags were immersed in two types of dissolution vessels: one containing 900 mL of simulated gastric juice (0.1 mol/L hydrochloric acid solution, HCl) and the other containing 900 mL of simulated intestinal juice (0.01 mol/L phosphate buffer solution, PBS, pH 7.4). All vessels were maintained at 37°C with a stirring speed of 100 rpm (Song, Yin *et al*., 2021). Following this, 2 mL samples were collected at specific time intervals (1, 5, 10, 15, 20, 30, 45, and 60 min) and an equivalent volume of dissolution medium was promptly added. Subsequently, the collected samples were filtered through a 0.45 μm micro porous filter and the GB content was assessed by LC-MS, using the methodology outlined in Section 2.8. The cumulative drug release percentage at each time point was then calculated. Three replicates were performed in parallel for each dissolution medium.

Stability study

The GB-NC freeze-dried powder was stored in a 10 mL glass vial and kept at 4ºC and 25ºC for 6 months. Samples were collected at 0, 1, 2, 3, 4, and 6 months to investigate the appearance, particle size and PDI of the GB-NC solution after redispersion.

Cellular permeability experiment

Cytotoxicity test

MDCK cells were cultured in DMEM (Dulbecco's Modified Eagle Medium) supplemented with 10% fetal bovine serum (FBS) and 1% penicillin-streptomycin, and incubated in a cell incubator maintained at 37°C, 5% CO_2, and 95% relative humidity. The medium was changed daily, and once cell confluency reached 80%–90%, enzymatic digestion was performed with 0.25% trypsin-EDTA solution. Cells were subcultured at a 1:4 split ratio to achieve the required cell density.

MDCK cells in the logarithmic growth phase were seeded into 96-well plates at a density of 5×10^3 cells per well and cultured for 24 hours. The GB suspension (dispersed in 0.5% PVP K30 aqueous solution) and GB-NC solution were diluted with DMEM to prepare drug-containing media with GB concentrations of 5, 10, 20, 40, 80, and 160 μM. The cells in the 96-well plates were then treated with the drug-containing media and further incubated for 2 hours. Additionally, cells treated with blank DMEM served as the negative control. Following incubation, the cells were washed three times with PBS buffer to remove any residual drug adhering to the cell surface. Subsequently, serum-free DMEM containing 10% CCK-8 reagent was added to each well. After a further 2 hours incubation, the absorbance of the supernatant at 450 nm was measured using an Infinite 200 Pro microplate reader (Tecan, Salzburg, Austria). The cell survival rate (%) was calculated using the formula below: Cell survival rate (%) = (Mean absorbance of experimental group / Mean absorbance of control group) × 100% (Tang, Liu *et al*., 2021).

Cellular permeability experiment

The Transwell chamber was placed on a 24-well plate, and MDCK cells were seeded into the upper chamber of the Transwell at a concentration of 1×10^5 cells/mL and a volume of 0.4 mL. Additionally, 1 mL of blank DMEM was added to the lower chamber. The 24-well plate was then placed in a 5% CO_2 incubator at 37°C, and the media were changed every other day. Transepithelial Electrical Resistance (TEER) values were measured on both sides of the Transwell membrane using a Millicell ERS electrical resistance meter (Merck Millipore, Billerica, USA). Once the TEER value exceeded 250 $\Omega\cdot cm^2$, the cell monolayer system was deemed suitable for subsequent experiments. Cells were cultured in Transwell chambers to form a monolayer. Prior to the experiment, the upper and lower chambers were rinsed three times with Hank's Balanced Salt Solution (HBSS) preheated to 37°C. Subsequently, DMEM was added to the chambers to dilute the GB suspension or GB-NC solution to a final concentration of 20 μM, thereby preparing the drug-containing working solution. Next, 200 μL of the drug-containing working solution was added to the upper chamber of each Transwell, while 1 mL of blank medium was added to the corresponding lower chamber to ensure that the liquid levels in both chambers were equal. The Transwell chambers were then placed in a 37°C incubator with 5% CO_2 for further incubation. After incubation for different time intervals (15, 30, 60, 90, and 120 min), 200 μL of the solution was collected from the lower chamber and transferred to an Eppendorf (EP) tube, followed by the addition of 200 μL of fresh medium to the lower tube. The concentration of GB in the samples at each time point was determined using the method outlined in Section 2.8. Based on this concentration data, the cumulative drug transport amount and apparent permeability coefficient (P_{app}) were calculated.

Statistical analysis

The experimental data were presented as the mean ± standard deviation (mean ± SD). Statistical significance of differences was analyzed using Student's t-test or one-way analysis of variance (ANOVA) with GraphPad Prism 9 (GraphPad Software Inc., La Jolla, CA, USA), with a significance level set at $P < 0.05$.

RESULTS

Quality by design approach

Initially, it was determined that the QTPP entails the formulation of an orally administered GB preparation with high drug loading, enhanced dissolution properties, good stability, and efficient absorption. Subsequently, the CQAs of the product were identified as particle size, PDI, and SI, and the corresponding monitoring metrics were defined. Lastly, based on the risk analysis of preliminary experimental results, the most critical CPPs identified included the stabilizer type, stabilizer concentration, and grinding time. Additionally, grinding speed were found to have a certain degree of influence on product CQAs. The effect of temperature on product quality mainly manifested in product stability, though the effect was negligible because an ice water bath was used during preparation. Given a fixed dosage of 20 mg per sample, the dosage-related risk was deemed low. Table 2 presents the QTPP and CQAs, along with their respective objectives and explanations. Furthermore, Table 3 presents the analysis of CPPs and their associated risk levels.

Screening of stabilizers

For this research, we selected twelve commonly used stabilizers in nanocrystal preparation, encompassing anionic surfactants, non-ionic surfactants, high molecular polymers, and surface-active natural products. The impact of various stabilizers on particle size, PDI, and stability is presented in Table 4. The findings indicated that employing PVP K30 as a stabilizer yielded GB-NC with smaller particle size and relatively high stability. Conversely, using SL as the stabilizer resulted in GB-NC with good stability but larger particle size. Thus, combining SL and PVP K30 was proposed to decrease particle size and enhance the stability of GB-NC.

Process parameters

In the preparation system of this study, the zirconia beads undergo rotation through the rotor, resulting in significant

mutual collisions and shear forces among the drug particles, grinding medium (zirconia beads), and the container wall. This process gradually reduces the size of solid particles to the nanometer scale, ultimately yielding drug nanocrystals. The particle size of the nanocrystals was found to be influenced by the diameter of the zirconia beads. As depicted in Fig. 2A, the particle size of GB-NC decreased with decreasing size of zirconia beads, and smaller zirconia beads facilitated a more rapid reduction in particle size. Consequently, to reduce particle size, 0.08–0.12 mm zirconia beads were selected for grinding. The magnitude of the shear force is intricately linked to the rotational speed of the rotor. Fig. 2B demonstrates the impact of rotational speed on both the particle size of GB-NC and PDI. When the rotational speed was below 1000 r/min, the zirconia beads failed to rotate fully, leading to a distinct height difference at the interface between the zirconia beads and the liquid medium. Consequently, the grinding process became insufficient, resulting in larger particle sizes of the prepared GB-NC. Conversely, when the rotational speed exceeded 1200 r/min, excessive speed caused the grinding bottle to shake. Additionally, the high heat generated by the rapid rotation increased the likelihood of GB-NC aggregation. As a result, both the particle size and PDI of GB-NC increased significantly. Thus, we ultimately selected a rotational speed of 1000 r/min.

Experimental optimization of GB-NC

The Box-Behnken Response Surface Method is a widely used experimental design and optimization approach that integrates the benefits of central composite design and response surface analysis. Its objective is to identify the optimal conditions with minimal experimental runs. In this study, the investigated factors were determined based on the risk analysis results of CPPs that affect CQAs. Specifically, the selected factors were PVP K30 concentration (X_1), SL concentration (X_2), and grinding time (X_3). To optimize the formulation and process of GB-NC, a Box-Behnken design with 3 factors and 3 levels was employed. A total of 17 experimental runs were conducted. The experimental design and results were presented in Table 5.

The obtained experimental data were analyzed using Design-Expert 11.0.4. The findings indicated that the relationship between the mean particle size (Y_1), PDI (Y_2), and SI (Y_3) (as response variables) and three independent factors—PVP K30 concentration (X_1), SL concentration (X_2), and grinding time (X_3)—can be described by a quadratic equation. The fitting equations were as follows:

(1) $Y_1 = 81.34 + 6.1 \times X_1 + 13.4 \times X_2 + 9.1 \times X_3 + 4.3 \times X_1X_2 - 3 \times X_1X_3 - 11.45 \times X_2X_3 + 39.75 \times X_1^2 + 27.85 \times X_2^2 + 136.71 \times X_3^2$

(2) $Y_2 = 0.1026 + 0.0025 \times X_1 + 0.0109 \times X_2 + 0.0064 \times X_3 - 0.004 \times X_1X_2 + 0.0025 \times X_1X_3 - 0.0233 \times X_2X_3 + 0.0291 \times X_1^2 + 0.0363 \times X_2^2 + 0.0838 \times X_3^2$

(3) $Y_3 = 0.9612 + 0.0236 \times X_1 + 0.1299 \times X_2 + 0.0092 \times X_3 - 0.0123 \times X_1X_2 + 0.001 \times X_1X_3 + 0.0005 \times X_2X_3 - 0.0465 \times X_1^2 - 0.0630 \times X_2^2 - 0.0892 \times X_3^2$

The P-values of the three fitting equations were all below 0.0001, indicating a high level of statistical significance. Additionally, the lack-of-fit P-values were all above 0.05, suggesting that the model adequately fit the data. Furthermore, both the R^2 and adjusted R^2 values exceeded 0.9, with a difference of less than 0.2 between them, indicating a strong correlation between the model response and the experimental data. These findings demonstrated that the aforementioned model was well-fit and accurately represented the GB-NC formulation and process. The results of the analysis of variance for response values are presented in Table 6.

Based on the fitting equations, the three-dimensional (3D) response surface plots were generated (Fig. 3A-I). The impact of grinding time on the particle size and PDI of GB-NC could be observed via equation fitting and the 3D plots. As the grinding time increased, the particle size and PDI of GB-NC initially decreased, followed by a gradual increase. The particle size and PDI were affected by the concentrations of PVP K30 and SL, demonstrating a gradual decline in both parameters as their concentration increased. Nevertheless, when the concentration exceeded the optimal level, it led to an increase in both particle size and PDI. Regarding the stability of the GB-NC, the concentration of SL had a significant influence on the SI. As the concentration of SL rose, the SI of GB-NC also increased. This finding was consistent with the results from the previous stabilizer screening experiments.

To define optimization targets, Design-Expert 11.0.4 software was utilized, considering the minimum average particle size (Y_1), minimum PDI (Y_2), and maximum SI (Y_3). The optimal process conditions were obtained as X_1 = 0.506%, X_2 = 0.343%, X_3 = 9.996 h. Based on the optimized parameters obtained, three batches of GB-NC were prepared, and their corresponding indices were measured, as are presented in Table 7. The results indicated a close agreement between the predicted and measured values, demonstrating a good predictive performance of the model.

Freeze-drying of GB-NC and screening of lyoprotectants

It was worth noting that the nanocrystal drug solution was prone to aggregation, precipitation, and other undesirable phenomena, rendering it unsuitable for transportation and long-term storage. To ensure long-term stability, the nanocrystals were freeze-dried in this study.

There were numerous variables that influenced the freeze-drying process, with lyoprotectants playing a crucial role in determining the quality of the final product. In this study, we examined the protective effects of five commonly used lyoprotectants (mannitol, xylitol, maltose, glucose, and glycine) on GB-NC. The findings are presented in Table 8. The experimental findings indicated that using glycine as a lyoprotectant yielded a final product that exhibited good

overall appearance, including a smooth surface and a porous texture. Additionally, a marginal increase in particle size was observed upon redispersion. When glucose was used as a lyoprotectant, the resulting product displayed suboptimal visual properties, but the particle size remained largely unchanged upon redispersion. As a result, we ultimately chose to use a combination of 3% glycine and 3% glucose as the lyoprotectants.

Characterization of optimized GB-NC

Fig. 4A and 4B illustrate that non-freeze-dried GB-NC appeared as a translucent solution, with no visible insoluble components or clumps. In contrast, the freeze-dried GB-NC powder exhibited a white cake-like appearance with a smooth and plump surface, and demonstrated good redispersibility. Fig. 4C and 4D display the TEM image of the GB-NC solution and SEM image of the freeze-dried GB-NC powder, respectively. TEM observation revealed that the GB-NC had an irregular shape, while SEM analysis showed that the freeze-dried GB-NC powder was composed of small nanoscale particles. Prior to freeze-drying, the particle size of GB-NC was measured to be 82.4 ± 1.97 nm, and the zeta potential was -12.5 ± 1.2 mV. Upon redispersion, the particle size of redispersed GB-NC increased slightly to 87.9 ± 1.4 nm, and the zeta potential decreased to -14.2 ± 2.1 mV. PXRD analysis was used to confirm the crystalline state of GB in the freeze-dried GB-NC powder. Fig. 5 illustrates the X-ray diffraction pattern of the GB raw material, revealing distinct and intense diffraction peaks indicating high crystallinity. Although the GB-NC freeze-dried powder retained the characteristic crystalline peaks, their intensity was slightly diminished, likely because the grinding process significantly reduced particle size of GB.

The behavior of dissolution in vitro

As shown in Fig. 6A and 6B, the cumulative dissolution of GB in 0.1 mol/L HCl over 2 hours was found to be 27%, whereas in PBS (pH 7.4), it was 45%. Notably, no significant difference was observed between the dissolution profiles of the lyophilized powder of the physical mixture and the bulk drug, suggesting that the addition of excipients alone did not enhance the drug's dissolution rate. However, the use of GB-NC demonstrated a substantial improvement in the drug's dissolution, with over 90% of the drug dissolved within 20 minutes in both 0.1 mol/L HCl and PBS (Hang, Hu *et al*., 2021).

Stability studies

The freeze-dried powder of GB-NC, as depicted in Fig. 7A and 7B, was stored at 4°C and 25°C for 6 months. Upon redissolution, the particle size and PDI remained relatively unchanged, indicating that the freeze-dried GB-NC product exhibited good stability and met the predetermined QTPP criteria.

Cellular permeability experiment

MDCK monolayer cells were used as a model of small intestinal epithelial cells to investigate the impact of GB-NC on drug transport across monolayer cells, thereby enabling inference of the drug's oral absorption potential (Wen, Gao *et al*., 2021). As shown in Fig. 8A, compared with the GB raw material suspension, the P_{app} of GB-NC exhibited a highly significant increase ($p < 0.001$). Meanwhile, as depicted in Fig. 8B, the cumulative transmembrane transport amount of GB-NC over time showed a significant increase ($p < 0.05$). However, despite these enhancement, the transmembrane transport rate of GB-NC decreased progressively over time. The findings indicate that GB-NC has the potential to enhance the transmembrane transport of drugs, with its transport rates diminishing as the concentration gradient across the cell membrane decreases.

DISCUSSION

The CQAs of the GB-NC product were identified as particle size, PDI, and SI. This identification was based on the Noyes-Whitney equation, which posits that a reduction in particle size leads to an increase in the total effective surface area of drug particles, thereby increasing the dissolution rate (Noyes and Whitney, 2002). Furthermore, according to the Oswald ripening mechanism (Voss and Haase, 2013), during the crystal nucleation and growth of GB-NC, the competitive growth of large particles is dependent on the assimilation of smaller particles. Consequently, maintaining a uniform size distribution in the GB-NC system can effectively impede this phenomenon and enhance the system's stability.

The selection of an appropriate stabilizer holds significant importance in reducing the particle size and PDI, and enhancing the stability of GB-NC (Zhang, Guan *et al*., 2022). Poloxamer 188, a non-ionic surfactant, stabilizes nanocrystals by providing steric hindrance (Tuomela, Hirvonen *et al*., 2016). The outcomes of this study unequivocally showed that Poloxamer 188 failed to form a stable GB-NC, indicating its limited ability to adsorb adequately onto drug particles and generate effective steric hindrance. Sodium dodecyl sulfate (SDS), an anionic surfactant, can adsorb onto the surface of drug nanoparticles through hydrophobic interactions. Using SDS as a stabilizer yielded a semi-transparent solution with smaller particle size. Nevertheless, the drug nanoparticles exhibited rapid aggregation and precipitation during the subsequent storage. This occurrence could be ascribed to the strong solubilizing effect of SDS on drugs, which expedites the Ostwald ripening process. This phenomenon, which encompasses the dissolution of smaller particles and the growth of larger particles, ultimately culminates in particle aggregation and precipitation. In contrast, the polymers HPMC E5 and PVP K30 could coat drug particles and provide spatial stability via hydrogen bonds (Douroumis and Fahr, 2007). The results indicated that both HPMC E5 and PVP K30 can effectively stabilize GB-NC with satisfactory stability.

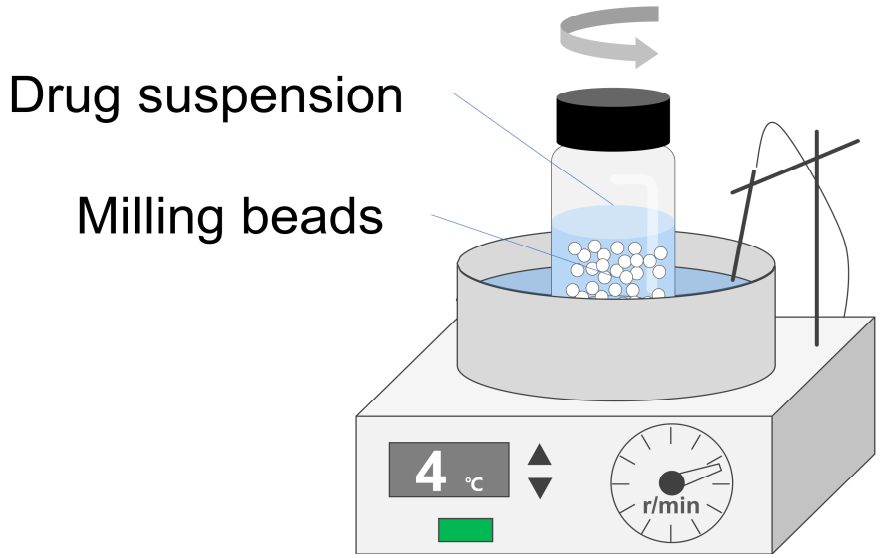

Fig. 1: Experimental device for preparing nanocrystals.

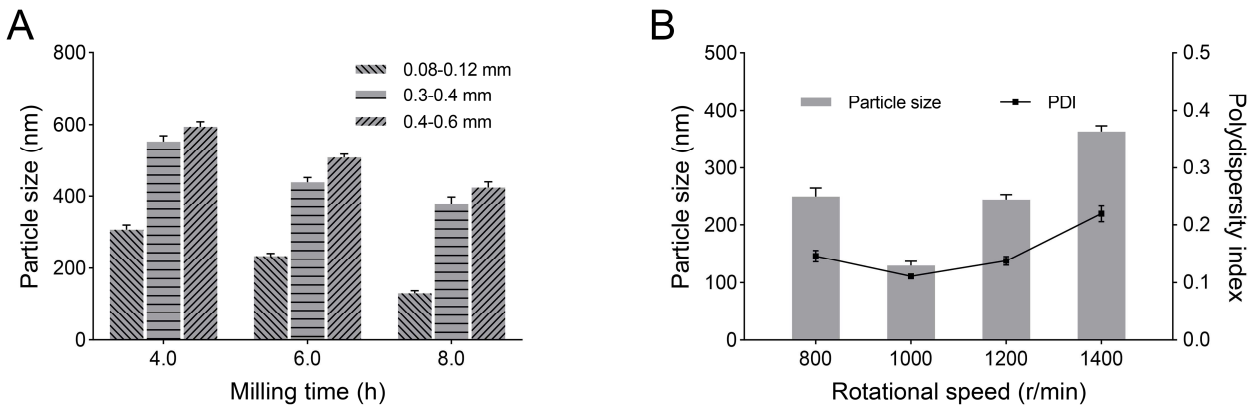

Fig. 2: Effect of (A) milling beads diameter and (B) rotational speed on the particle size and PDI of nanocrystals.

Table 1: Factors and response variables of the Box-Behnken design.

Factors	Low limit	High limit
X_1: PVPK30 concentration （w/v, %）	0.1	0.9
X_2: SL concentration （w/v, %）	0.1	0.5
X_3: Milling time （h）	4	16
Responses	Goal	
Y_1: Particle size (nm)	minimize	
Y_2: PDI	minimize	
Y_3: SI	maximize	

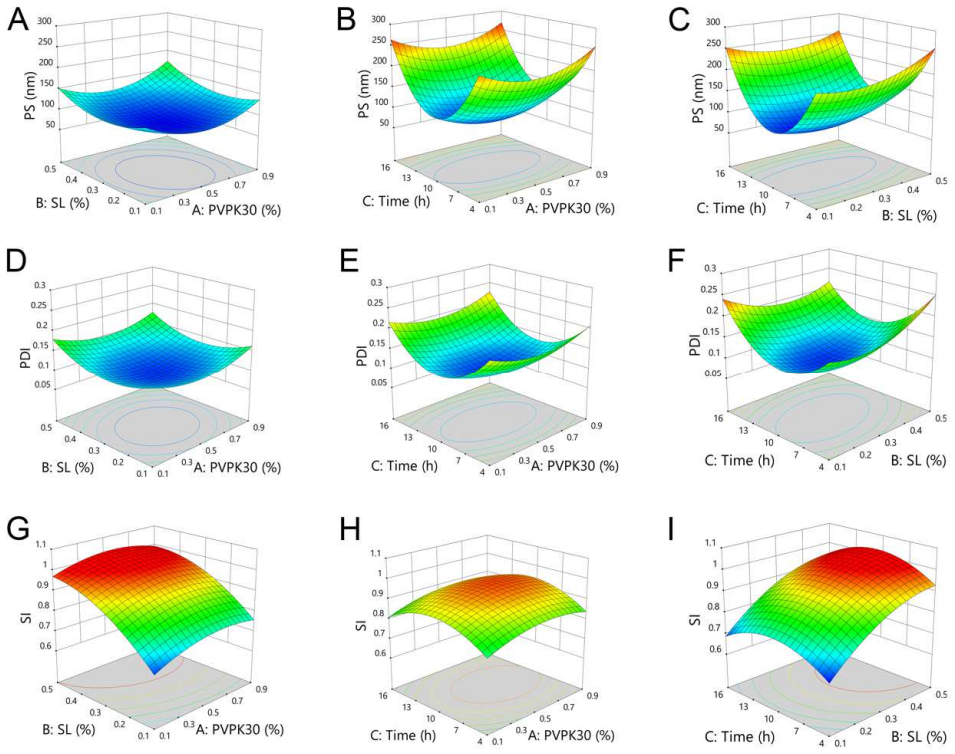

Fig. 3: Response surface profiles show the effects of PVP K30 concentration (X_1), SL concentration (X_2), and milling time (X_3) on (A-C) particle size (PS, Y_1), (D-F) PDI (Y_2), and (G-I) SI (Y_3) of GB-NC.

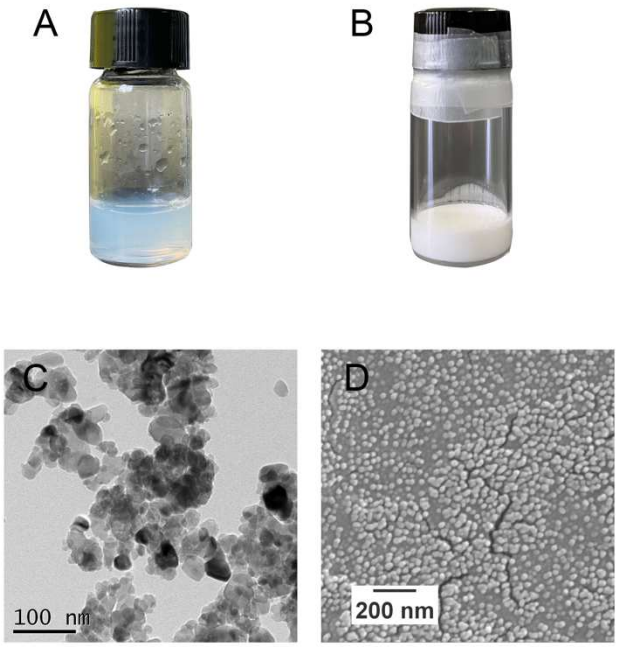

Fig. 4: (A) GB-NC solution. (B) Lyophilized GB-NC powder. (C) TEM image of GB-NC solution. (D) SEM image of lyophilized GB-NC powder.

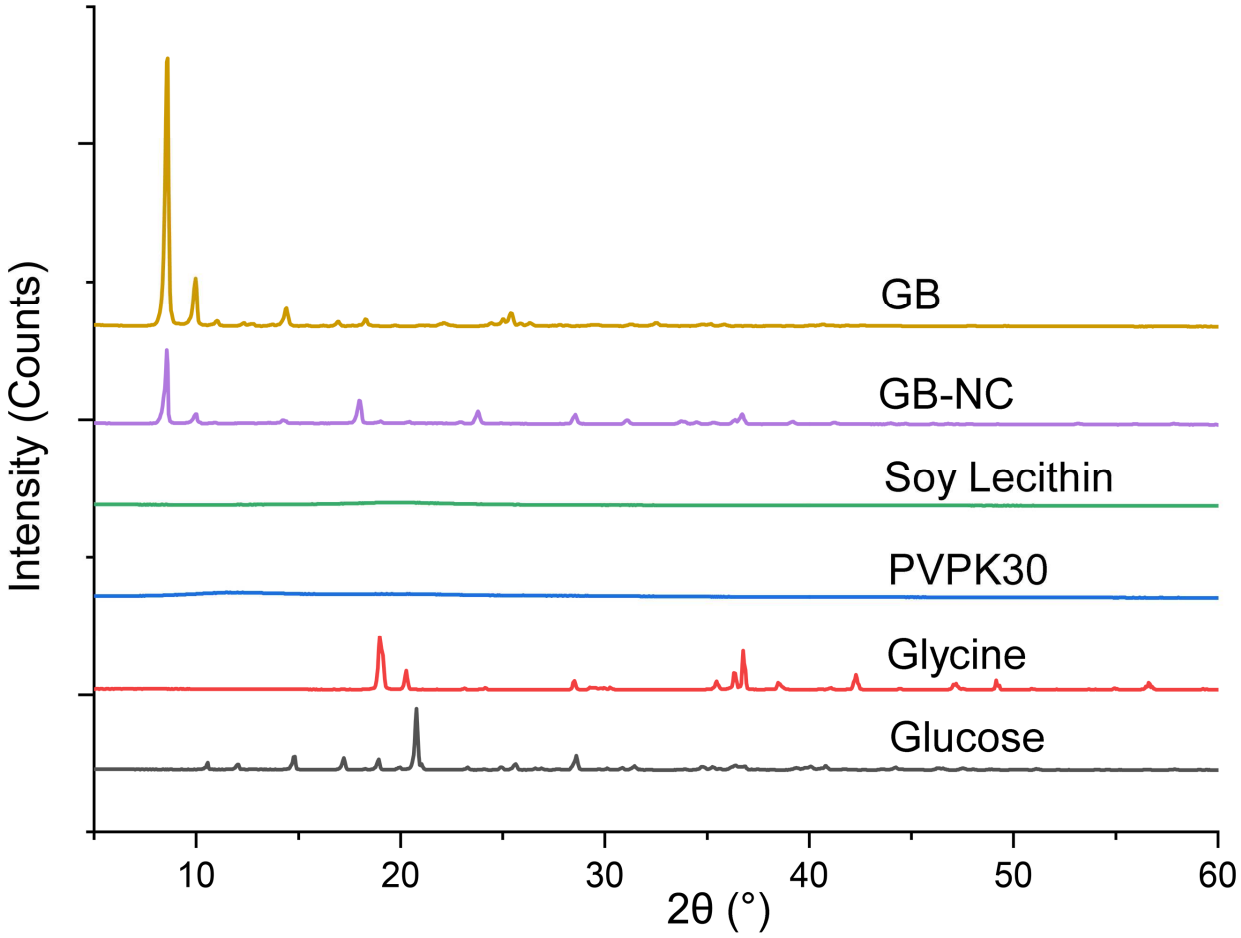

Fig. 5: PXRD patterns of GB crude powder, lyophilized GB-NC powder and excipients.

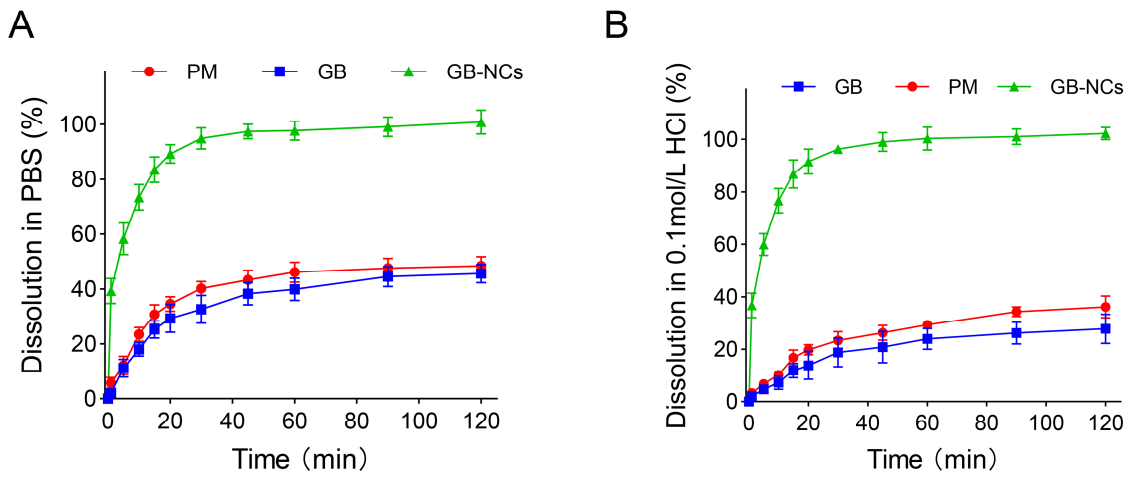

Fig. 6: Dissolution profiles of GB crude drug, physical mixture and lyophilized GB-NC in (A) PBS (pH 7.4) and (B) 0.1 mol/L HCl solution (mean ± SD, n = 3).

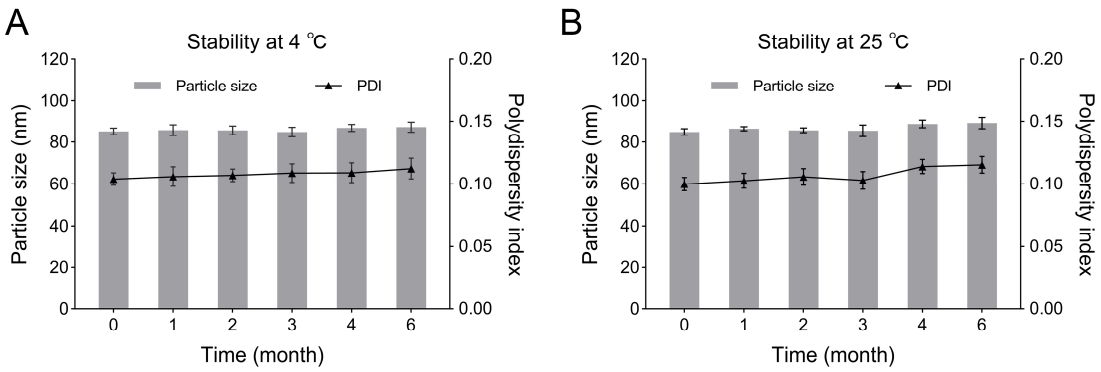

Fig. 7: Stability of lyophilized GB-NC powder stored at 4 ℃ (A) and 25 ℃ (B) (mean ± SD, n = 3).

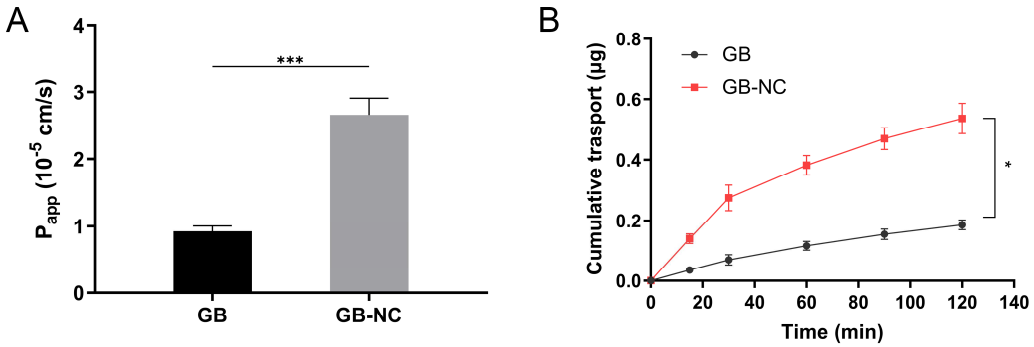

Fig. 8: (A) P_{app} of GB suspension and GB-NC solution across MDCK cell monolayers. (B) Cumulative cellular permeability of GB suspension and GB-NC solution over time. (mean ± SD, n = 6, *$p < 0.05$, ***$p < 0.001$)

Table 2: QTPP and CQA for GB-NC.

QTPP	Target	Justification
Formulation	Nanocrystals freeze-dried powder	a. Drug nanocrystals lack carriers, possess favorable safety profiles, and exhibit high drug loading capacities. b. Using nanocrystals in drug preparation can enhance drug solubility and dissolution, thereby leading to improved oral bioavailability. c. Freeze-drying technology for solidifying nanocrystals enhances their storage stability.
Route of administration	Oral	Oral administration is the preferred route for long-term treatment.
Dosage strength	20 mg/mL	The typical clinical dosage ranges from 20 to 60 mg per day.
Dissolution	Higher than plain drug	Increased dissolution aids in drug absorption within the gastrointestinal tract.
Stability	At least 6 months	The stability of pharmaceutical preparations is crucial for ensuring their clinical efficacy and safety.
Absorption	Better than plain drug	Improving the oral absorption of drugs helps enhance therapeutic efficacy
CQAs	Target	Justification
Particle size	Nanometer scale, the smaller the better	Enhanced solubility and dissolution can be achieved by using smaller particle sizes.
PDI	Less than 0.2	The uniform distribution of particle size not only enhances system stability but also plays a crucial role in determining the drug's safety and efficacy.
SI	Greater than 0.8	The stability coefficient serves as a valuable metric for assessing the stability of the preparations.

Table 3: Risk assessment for GB-NC formulations.

CPPs	Risk level Particle size	PDI	SI
Drug concentration[a]	Low	Low	Low
Stabilizer type	High	High	High
Stabilizer concentration	High	High	High
Diameter of milling beads	High	Low	Low
Milling speed	Medium	Low	Low
Milling time	High	High	High
Temperature	Low	Low	Medium

[a]Drug concentration was fixed with 20 mg/mL.

Table 4: Effect of different stabilizers on average particle size, PDI, and stability (mean ± SD, n = 3).

Stabilizer	Particle Size (nm)	PDI	Stability（at room temperature）
Poloxamer 188	ND	ND	precipitation immediately
Poloxamer 407	ND	ND	precipitation immediately
HS-15	936.0±16.0	0.536±0.035	precipitation appeared within 4 hours
TPGS	884.9±9.0	0.422±0.024	precipitation appeared within 4 hours
EL-35	815.1±11.3	0.352±0.023	precipitation appeared within 4 hours
Tween 80	846.9±10.1	0.361±0.026	precipitation appeared within 4 hours
SDC	316.7±6.0	0.265±0.011	precipitation appeared within 4 hours
SDS	331.9±6.2	0.221±0.013	precipitation appeared within 4 hours
HPMC E5	613.2±6.5	0.339±0.017	unchanged within 24 hours
PVP K30	348.0±7.8	0.240±0.018	unchanged within 24 hours
GLA	884.7±13.3	0.351±0.024	unchanged within 24 hours
SL	637.1±7.6	0.358±0.019	unchanged within 48 hours

ND means the data could not be obtained because the samples precipitated immediately.

Table 5: Experimental compositions and observed responses from the Box-Behnken design.

Run	Factors			Responses		
	X_1: (w/v, %)	X_2: (w/v, %)	X_3: (h)	Y_1: (nm)	Y_2:	Y_2:
1	0.1	0.3	16	264.7	0.217	0.811
2	0.9	0.3	16	270.1	0.231	0.857
3	0.1	0.1	10	132.3	0.153	0.691
4	0.5	0.3	10	83.2	0.109	0.954
5	0.9	0.1	10	136.7	0.162	0.766
6	0.1	0.3	4	239.5	0.205	0.796
7	0.5	0.5	4	261.1	0.253	0.935
8	0.5	0.3	10	80.2	0.105	0.965
9	0.5	0.5	16	255.4	0.215	0.956
10	0.5	0.1	16	253.6	0.239	0.682
11	0.1	0.5	10	152.6	0.182	0.962
12	0.9	0.5	10	174.2	0.175	0.988
13	0.5	0.3	10	82.6	0.093	0.967
14	0.9	0.3	4	256.9	0.209	0.838
15	0.5	0.1	4	213.5	0.184	0.663
16	0.5	0.3	10	78.4	0.097	0.952
17	0.5	0.3	10	82.3	0.109	0.968

Table 6: Summary of the analysis of variance (ANOVA) for response variables.

	Source	Y_1	Y_2	Y_3
P-value	Model	< 0.0001	< 0.0001	< 0.0001
	X_1	< 0.0001	0.3008	0.0002
	X_2	< 0.0001	0.0018	< 0.0001
	X_3	< 0.0001	0.0247	0.0262
	X_1X_2	0.0036	0.2467	0.0339
	X_1X_3	0.02	0.4555	0.8361
	X_2X_3	< 0.0001	0.0002	0.9175
	X_1^2	< 0.0001	< 0.0001	< 0.0001
	X_2^2	< 0.0001	< 0.0001	< 0.0001
	X_3^2	< 0.0001	< 0.0001	< 0.0001
	Lack of Fit	0.4742	0.7387	0.2334
R^2	R^2	0.9997	0.9939	0.9971
	Adjusted R^2	0.9993	0.986	0.9933
	Predicted R^2	0.9977	0.9686	0.9691

Table 7: Predicted and observed values of the optimal GB-NC formulation (mean ± SD, n = 3).

Responses	Importance	Predicted values	Observed values
Y_1: Particle size (nm)	++++	85.535	82.4 ± 1.97
Y_2: PDI	++++	0.107	0.102 ± 0.010
Y_3: SI	++++	0.986	0.984 ± 0.011

Table 8: Evaluation results of GB-NCs with different cryoprotectants.

Cryoprotectants	Appearance	Redispersion	SR
None	+	-	ND
Mannitol	++	+	3.95
Xylitol	-	-	ND
Glucose	-	+	1.02
Maltose	+	+	ND
Glycine	++	+	1.63

Appearance: ++ means compacted and smooth cake, no collapse and atrophy; + means cake with slightly shrink, no obvious collapse and atrophy; - means non-cake, collapse and atrophy critically. Redispersion: + means easy to redispersion (less than 30s); - means hard to redispersion (more than 30s); ND means the data could not be obtained because the reconstituted samples precipitated immediately.

Nevertheless, when compared to PVP K30, GB-NC prepared using HPMC E5 had a larger particle size, likely due to the higher viscosity of HPMC E5 solution, which resulted in insufficient grinding efficiency (Ghosh, Schenck *et al*., 2013). A stable GB-NC could be formed using SL, which is attributed to the amphiphilic properties of SL that enable strong hydrophobic interactions with GB molecules, leading to the formation of a phospholipid membrane on the drug surface (Wang, Cao *et al*., 2019).

It is commonly accepted that the minimum achievable particle size of nanocrystals is approximately 1000-fold smaller than the diameter of the milling beads (Romero, Keck *et al*., 2016). For instance, the use of 0.1 mm milling beads could yield nanocrystals of approximately 100 nm. In this study, 0.08–0.1 mm milling beads were used, resulting in nanocrystals with a final particle size of approximately 90 nm. Excessive grinding time could result in a particle size increase, which is attributed to the ongoing grinding process that continuously reduces drug particle size. Smaller particles have higher surface energy, thereby increasing the likelihood of secondary agglomeration and subsequently leading to particle size increase (Romero, Keck *et al*., 2016).

While our previous study demonstrated that the nanocrystals self-stabilized Pickering nanoemulsion of GB outperformed conventional nanocrystals in terms of oral bioavailability and therapeutic efficacy, the practical challenges of scaling up Pickering nanoemulsions for industrial production could not be overlooked. These challenges include complex manufacturing processes, high stabilizer costs, and limited batch-to-batch reproducibility. In contrast, the nanocrystal formulation developed in this work offers a more cost-effective and scalable solution for industrial applications. The experimental results substantiated the advantages of this nanocrystal formulation: they exhibited significantly enhanced

dissolution rates (>90% within 20 minutes), superior cellular permeability (apparent permeability coefficient: $2.3 \pm 0.3 \times 10^{-6}$ cm/s), and improved stability compared to GB raw material. Unlike our prior research, which focused on mechanistic comparisons between Pickering nanoemulsions and nanocrystals, this study systematically addressed the formulation design and process optimization of GB nanocrystals through a Quality by Design (QbD) approach. By employing a miniaturized wet bead milling technique, we achieved precise control over particle size (82.4 ± 1.97 nm) and stability while ensuring scalability for large-scale oral formulation development. This work highlighted the practicality of nanocrystals as a commercially viable strategy to overcome the limitations of poorly soluble drugs like GB, balancing therapeutic performance with industrial feasibility.

CONCLUSION

This research successfully developed GB-NC through a miniaturized wet bead milling method guided by QbD principles, resulting in the optimized particle size and stability of GB-NC. The GB-NC exhibited an increased dissolution rate and enhanced cellular permeability, which indicates its potential to improve oral bioavailability. While these results laid the foundation for the future development of GB-NC as a promising formulation to enhance therapeutic effectiveness, further studies are needed to fully evaluate large-scale manufacturing challenges. Future research should focus on scaling up production, long-term stability testing, and investigating the degradation kinetics of GB-NC. Additionally, in vivo pharmacokinetic studies will be crucial to confirm the therapeutic potential of GB-NC as a promising formulation for poorly soluble drugs like GB.

Acknowledgment
The authors wish to express their deepest appreciation to Professor Lan Cheng from the College of Pharmacy, Liaoning University of Traditional Chinese Medicine, for her instrumental role in shaping the study design. Her profound expertise in experimental strategy development and critical evaluation of research frameworks significantly enhanced the scientific validity and innovation of this study.

Authors' contributions
Y. L.: Conceptualization, Project administration, Methodology, Formal analysis, Data curation, Funding acquisition, Writing. H. X.: Methodology, Data curation, Resources. H. W.: Investigation, Data curation. M. L.: Investigation, Data curation. All authors read and approved the final manuscript.

Funding
This work was financially supported by the Liaoning Provincial Department of Education Basic Scientific Research Project (Grant No.: LJ242414289010, PI: Yun Liu); and the Liaoning Provincial Doctoral Research Initiation Fund Project (Grant No.: 2025-BS-0926, PI: Yun Liu).

Data availability statement
The datasets used and analysed during the current study are available from the corresponding author on reasonable request.

Ethical approval
Not applicable

Conflict of interest
The authors declare no conflict of interest.

REFERENCES

Aa L, Fei F, Tan Z, Aa J, Wang G and Liu C (2018). The pharmacokinetics study of ginkgolide A, B and the effect of food on bioavailability after oral administration of ginkgolide extracts in beagle dogs. *Biomed. Chromatogr.* **32**(6): e4212.

Almutairi FM, Ullah A, Althobaiti YS, Irfan HM, Shareef U, Usman H and Ahmed S (2022). A review on therapeutic potential of natural phytocompounds for stroke. *Biomedicines,* **10**(10): 2566.

Che J, Fu Y, Li Y, Zhang Y, Yin T, Gou J, Tang X, Wang Y and He H (2024). Eudragit L100-coated nintedanib nanocrystals improve oral bioavailability by reducing drug particle size and maintaining drug supersaturation. *Int. J. Pharm.,* **658**: 124196.

Cheng M, Yuan F, Liu J, Liu W, Feng J, Jin Y and Tu L (2020). Fabrication of fine puerarin nanocrystals by box-behnken design to enhance intestinal absorption. *AAPS Pharm. Sci. Tech.,* **21**(3): 90.

Douroumis D and Fahr A (2007). Stable carbamazepine colloidal systems using the cosolvent technique. *Eur. J. Pharm. Sci.* **30**(5): 367-374.

Farooqi S, Yousuf RI, Shoaib MH, Ahmed K, Ansar S and Husain T (2020). Quality by design (QbD)-Based numerical and graphical optimization technique for the development of osmotic pump controlled-release metoclopramide HCl tablets. *Drug Des. Devel. Ther.* **14**: 5217-5234.

Feng Z, Sun Q, Chen W, Bai Y, Hu D and Xie X (2019). The neuroprotective mechanisms of ginkgolides and bilobalide in cerebral ischemic injury: A literature review. *Mol. Med.,* **25**(1): 57.

Gachowska M, Szlasa W, Saczko J and Kulbacka J (2021). Neuroregulatory role of ginkgolides. *Mol. Biol. Rep.,* **48**(7): 5689-5697.

Ghosh I, Schenck D, Bose S, Liu F and Motto M (2013). Identification of critical process parameters and its interplay with nanosuspension formulation prepared by top down media milling technology--a QbD perspective. *Pharm. Dev. Technol.,* **18**(3): 719-729.

Hang L, Hu F, Shen C, Shen B, Zhu W and Yuan H (2021). Development of herpetrione nanosuspensions stabilized by glycyrrhizin for enhancing bioavailability and synergistic hepatoprotective effect. *Drug Dev. Ind. Pharm.,* **47**(10): 1664-1673.

Khan MA, Ansari MM, Arif ST, Raza A, Choi HI, Lim CW, Noh HY, Noh JS, Akram S, Nawaz HA, Ammad M, Alamro AA, Alghamdi AA, Kim JK and Zeb A (2021). Eplerenone nanocrystals engineered by controlled crystallization for enhanced oral bioavailability. *Drug Deliv.,* **28**(1): 2510-2524.

Kuk DH, Ha ES, Ha DH, Sim WY, Lee SK, Jeong JS, Kim JS, Baek IH, Park H, Choi DH, Yoo JW, Jeong SH, Hwang SJ and Kim MS (2019). Development of a resveratrol nanosuspension using the antisolvent precipitation method without solvent removal, based on a quality by design (QbD) approach. *Pharmaceutics,* **11**(12): 688.

Lestari MLAD, Müller RH and Moschwitzer JP (2015). Systematic screening of different surface modifiers for the production of physically stable nanosuspensions. *J. Pharm. Sci.,* **104**(3): 1128-1140.

Liu D, Galvanin F and Yu Y (2018). Formulation screening and freeze-drying process optimization of ginkgolide b lyophilized powder for injection. *AAPS Pharm. Sci. Tech.,* **19**(2): 541-550.

Liu T, Yao G, Liu X and Yin H (2017). Preparation nanocrystals of poorly soluble plant compounds using an ultra-small-scale approach. *AAPS Pharm. Sci. Tech.,* **18**(7): 2610-2617.

Liu Y, Liu W, Xiong S, Luo J, Li Y, Zhao Y, Wang Q, Zhang Z, Chen X and Chen T (2020). Highly stabilized nanocrystals delivering ginkgolide B in protecting against the Parkinson's disease. *Int. J. Pharm.,* **577**: 119053.

Liu Y, Zhang C, Cheng L, Wang H, Lu M and Xu H (2024). Enhancing both oral bioavailability and anti-ischemic stroke efficacy of ginkgolide B by preparing nanocrystals self-stabilized Pickering nano-emulsion. *Eur. J. Pharm. Sci.,* **192**: 106620.

Lu Y, Li Y and Wu W (2016). Injected nanocrystals for targeted drug delivery. *Acta. Pharm. Sin. B.,* **6**(2): 106-113.

Madgula VL, Avula B, Yu YB, Wang YH, Tchantchou F, Fisher S, Luo Y, Khan IA and Khan SI (2010). Intestinal and blood-brain barrier permeability of ginkgolides and bilobalide: *In vitro* and *in vivo* approaches. *Planta. Med.,* **76**(6): 599-606.

Mohammady M, Mohammadi Y and Yousefi G (2020). Freeze-drying of pharmaceutical and nutraceutical nanoparticles: The effects of formulation and technique parameters on nanoparticles characteristics. *J. Pharm. Sci.,* **109**(11): 3235-3247.

Noyes AA and Whitney WR (2002). The rate of solution of solid substances in their own solutions. *J. Am. Chem. Soc.*, **19**(12): 930-934.

Peters L, Dyer M, Schroeder E and D'Souza MS (2023). Invega hafyera (Paliperidone Palmitate): Extended-release injectable suspension for patients with schizophrenia. *J. Pharm. Technol.,* **39**(2): 88-94.

Romero GB, Keck CM and Muller RH (2016). Simple low-cost miniaturization approach for pharmaceutical nanocrystals production. *Int. J. Pharm.,* **501**(1-2): 236-244.

Song Z, Yin J, Xiao P, Chen J, Gou J, Wang Y, Zhang Y, Yin T, Tang X and He H (2021). Improving breviscapine oral bioavailability by preparing nanosuspensions, liposomes and phospholipid complexes. *Pharmaceutics,* **13**(2): 132.

Suzuki T, Taketomi Y, Yanagida K, Yoshida-Hashidate T, Nagase T, Murakami M, Shimizu T and Shindou H (2025). Re-evaluation of the canonical PAF pathway in cutaneous anaphylaxis. *Biochim. Biophys. Acta. Mol. Cell Biol. Lipids.,* **1870**(1): 159563.

Taki E, Soleimani F, Asadi A, Ghahramanpour H, Namvar A and Heidary M (2022). Cabotegravir/Rilpivirine: The last FDA-approved drug to treat HIV. *Expert Rev. Anti. Infect. Ther.,* **20**(8): 1135-1147.

Tang XY, Liu YM, Bai XL, Yuan H, Hu YK, Yu XP and Liao X (2021). Turn-on fluorescent probe for dopamine detection in solutions and live cells based on in situ formation of aminosilane-functionalized carbon dots. *Analytica. Chimica. Acta.,* **1157**.

Tuomela A, Hirvonen J and Peltonen L (2016). Stabilizing agents for drug nanocrystals: Effect on bioavailability. *Pharmaceutics,* **8**(2): 16.

Upton JEM, Grunebaum E, Sussman G and Vadas P (2022). Platelet activating factor (PAF): A mediator of inflammation. *Biofactors,* **48**(6): 1189-1202.

Voss B and Haase M (2013). Intrinsic focusing of the particle size distribution in colloids containing nanocrystals of two different crystal phases. *ACS Nano.,* **7**(12): 11242-11254.

Wang P, Cao X, Chu Y and Wang P (2019). Ginkgolides-loaded soybean phospholipid-stabilized nanosuspension with improved storage stability and *in vivo* bioavailability. *Colloids. Surf B. Biointerfaces.,* **181**: 910-917.

Wen J, Gao X, Zhang Q, Sahito B, Si H, Li G, Ding Q, Wu W, Nepovimova E, Jiang S, Wang L, Kuca K and Guo D (2021). Optimization of tilmicosin-loaded nanostructured lipid carriers using orthogonal design for overcoming oral administration obstacle. *Pharmaceutics,* **13**(3): 303.

Yang M, Wei X, Pan K, Zhou Z, Liu Y, Lv X and Yang B (2023). Brain-targeted ginkgolide B-modified carbonized polymer dots for alleviating cerebral ischemia reperfusion injury. *Biomater. Sci.,* **11**(11): 3998-4008.

Yang P, Cai X, Zhou K, Lu C and Chen W (2014). A novel oil-body nanoemulsion formulation of ginkgolide B: pharmacokinetics study and *in vivo* pharmacodynamics evaluations. *J. Pharm. Sci.,* **103**(4): 1075-1084.

Yue PF, Li Y, Wan J, Wang Y, Yang M, Zhu WF, Wang

CH and Yuan HL (2013). Process optimization and evaluation of novel baicalin solid nanocrystals. *Int. J. Nanomedicine.,* **8**: 2961-2973.

Zekri O, Boudeville P, Genay P, Perly B, Braquet P, Jouenne P and Burgot JL (1996). Ionization constants of ginkgolide B in aqueous solution. *Anal. Chem.,* **68**(15): 2598-2604.

Zhang G, Guan H, Li J, Li M, Sui X, Tian B, Dong H, Liu B, He Z, Li N, Zhao M and Fu Q (2022). Roles of effective stabilizers in improving oral bioavailability of naringenin nanocrystals: Maintenance of supersaturation generated upon dissolution by inhibition of drug dimerization. *Asian J. Pharm. Sci.,* **17**(5): 741-750.

Zhao J, Geng T, Wang Q, Si H, Sun X, Guo Q, Li Y, Huang W, Ding G and Xiao W (2015). Pharmacokinetics of Ginkgolide B after oral administration of three different ginkgolide b formulations in beagle dogs. *Molecules.,* **20**(11): 20031-20041.

Zhao Y, Xiong S, Liu P, Liu W, Wang Q, Liu Y, Tan H, Chen X, Shi X, Wang Q and Chen T (2020). Polymeric nanoparticles-based brain delivery with improved therapeutic efficacy of ginkgolide b in parkinson's disease. *Int. J. Nanomedicine.,* **15**: 10453-10467.